Observation of Temperature Profiles of Kototabang (Bukittinggi-West Sumatera Indonesia) Using Radiosonde and Rain Event Identification
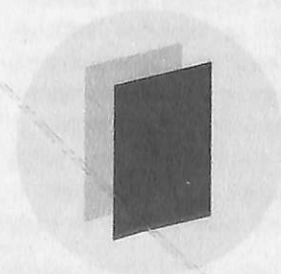
View the article online for updates and enhancements.

Observation of Temperature Profiles of Kototabang (Bukittinggi-West Sumatera Indonesia) Using Radiosonde and Rain Event Identification

I Juaeni[1], G. A Nugroho[1], S. A Rahayu[1], Safrijon[2], Halimurrahman[1]

[1]Center of Atmospheric Science and Technology
Indonesian National Institute of Aeronautics and Space (LAPAN)
Jln. Dr. Djundjunan No. 133, Bandung 40173, Indonesia

[2]Atmosphere and Space Observation Station Agam District, National Institute of Aeronautics and Space (LAPAN), Kototabang, West Sumatera, Indonesia

E-mail: inajuaeni@yahoo.com

Abstract. We recorded temperature profiles of Kototabang (West Sumatera- Indonesia) in a four days observation using Radio Acoustic Sounding System (RASS) and Radiosonde. The activity was carried out in August 2016, on a research cooperation framework of National Institute of Aeronautics and Space (LAPAN), Indonesia and Research Institute for Sustainable Humanosphere (RISH), Kyoto University, Japan. The current article discussed the temperature profile based on 12 times launch of Radiosonde, Convective Available Potential Energy (CAPE) estimation and its relationship with rain events, while the temperature profile based on RASS was discussed in another report. CAPE is the amount of energy an air parcel would have if lifted to a certain distance vertically through the atmosphere. CAPE is effectively the positive buoyancy of an air parcel and is an indicator of atmospheric instability, related to convection clouds. If there is not enough water vapour present, there is no ability for condensation, and therefore, storms, clouds, and rain will not form. CAPE is calculated as the area of positive region in the thermodynamic diagram or through relationships with virtual temperature. On August 30, 2016, at 08 LT, the range of temperatures based on Radiosonde measurements was recorded from 294.9°K at ground level to 186.5° K at an altitude of 26.8 km. The temperature range varied with time. CAPE based on Radiosonde data ranged from 0 to 5075.2 Jkg^{-1} within 30 August 2016 until 2 September 2016. The maximum CAPE value occurred on August 30, 2016 at 15.34 LT. Large CAPE (> 2000 Jkg^{-1}) was coincident with rain events.

1. Introduction

Climate and weather observations are essential for climate change policies and the development of weather services to improve the quality of public life. Progress and reliability in upper air measurements are important for the improvement and the validation of climate model and for numerical weather prediction (NWP).

Some challenges emerge and evolve dynamically, and up to now, an accurate solution regarding those issues is yet to be found. The issues are derived from variable atmosphere of upper air measurements, i.e. climate change issues based on temperature trends, which is important to assess each of atmospheric level, especially the troposphere, the stratosphere, the changes of temperature

trends [1-6], troposphere-stratosphere exchange [7-8], and dehydration of the stratosphere [6]. Both single observations with each instrument and a campaign involving many institutions and instruments have been employed in order to answers the problems. Not only research-based observation data, but also the radiosonde data is necessary as the input data and as the main part of the validation of NWP model [4, 9-13].

Recent developments of the technology for conventional (in situ) observation have led to significant improvement in measurement, processing, and transmission while at the same time, it has been able to reduce the expenditure and running cost of ground-based upper air network. Improvements in numerical weather and climate models need observations of atmospheric variables, such as clouds, winds, temperature, and humidity at the increasingly high resolution in space and time. Measurement of the variability of observed quantity at the models' resolved scales allows an optimal assimilation of the information by giving an estimation of the representative error. Interaction of different scales from global to convective scale is important in understanding atmospheric and climate physical process. Information of these interactions needs the data that include high spatial and time resolution from many regions. The future trend of weather forecasting and climate modelling is to optimize operational cost by mixing some existing in situ measurements (balloon-borne radiosondes, aircraft) with integrated ground-based remote sensing systems that provide a continuous sampling of the essential atmospheric variables in complement to satellite observation.

The current paper study discussed the minor part of the afore mentioned atmospheric physics research, through the temperature profiles at Kototabang (West Java-Sumatra, Indonesia) from Vaisala Radiosonde RS-41SG, as Radiosonde new generation has to improve on a level of in-situ observation accuracy and quality. This paper provide additional information on the latest temperature profile in the tropics and its relationship with Radiosonde indices. This research is was carried out in close collaboration between National Institute of Aeronautics and Space (LAPAN), Indonesia and Indonesia and Research Institute for Sustainable Humanosphere (RISH), Kyoto University, -Japan. This paper discusses the temperature profile based on 12 times Radiosonde launch and its relationship with some radiosonde indices, while the temperature profile based on Radio Acoustic Sounding System (RASS) is discussed in another report (in the process of publication).

2. Methods

The temperature profile at Equatorial Atmosphere Radar (EAR) site (Kototabang, West Sumatera, Indonesia) obtained from VAISALA/MW41 Sounding System, RS41-SG, S/N:M2720118 (**Figure 1**) was launched three times a day on the experiments period of August 30th, 2016 to September 2nd, 2016. The surface meteorology information was required for every launch, i.e pressure, temperature, humidity, wind direction, wind speed, latitude, longitude, and altitude of the site. EAR site positional information is shown in **Table 1**.

Table 1. Station position

	Longitude	Latitude	Altitude
EAR site at Koto Tabang (West Sumatera-Indonesia)	0.20°S	100.32°E	857.46 m

Radiosonde provides the profile of pressure, temperature, humidity, as well as wind direction. There are some indices that are evaluated from Radiosonde data. Some of the indices used in this paper are Convective Available Potential Energy (CAPE), a height of Equilibrium Level (EL), a pressure of EL and temperature of EL. CAPE is the amount of energy an air parcel would have if lifted a certain distance vertically through the atmosphere. CAPE is effectively the positive buoyancy of an air parcel and is an indicator of atmospheric instability related to convection clouds. In case there is not enough water vapour present, there is no ability for condensation, storms, clouds, and rain. CAPE is

calculated as the positive area in the thermodynamic diagram or through relationships with virtual temperature as in equation (1).

$$CAPE = \int_{z_f}^{z_n} g \left(\frac{T_{v,parcel} - T_{v,env.}}{T_{v,env.}} \right) dz \tag{1}$$

Where:
- z_f is the height of the level of free convection,
- z_n is the height of the equilibrium level (neutral buoyancy).
- $T_{v,parcel}$ is the virtual temperature of the specific parcel,
- $T_{v,env.}$ is the virtual temperature of the environment.
- g is the acceleration due to gravity.

Rainfall data from METEK Micro Rain Radar (MRR-2) and satellite images from HIMAWARI-8, IR-1 channel (http://weather.is.kochi-u.ac.jp/sat/gms.sea/) are used to expand the analysis. Statistical evaluation includes mean, standard deviation, and coefficient of correlation for 12 of data profile is used for common equation. Temperature deviation and coefficient of correlation are shown in equation (2) and equation (3), respectively.

$$\sigma T = T - \bar{T} \tag{2}$$

where:
- σT = temperature deviation
- T = temperature at certain time
- $\bar{T}$ = mean temperature

$$r_{xy} = \frac{\sum_{i=1}^{n}(x_i - \bar{x})(y_i - \bar{y})}{\sqrt{\sum_{i=1}^{n}(x_i - \bar{x})^2 \sum_{i=1}^{n}(y_i - \bar{y})^2}} \tag{3}$$

where:
- Σ is sigma, the symbol for sum up
- $x_i - \bar{x}$ is each x-value minus the mean of x
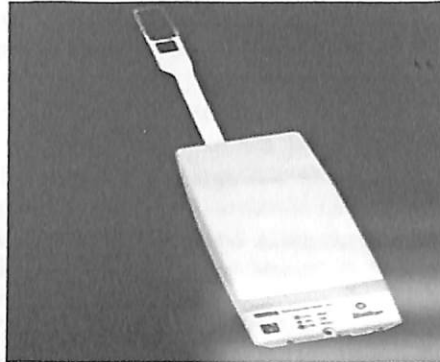- $y_i - \bar{y}$ is each y-value minus the mean of y

Figure 1. Vaisala Radiosonde RS41-SG and temperature sensor [14]

3. Results

3.1 Diurnal variation and mean temperature

On August 30th, 2016, at 08 LT, temperatures based on Radiosonde measurements ranged from 294.9K at ground level to 186.5 K at an altitude of 26.8 km. The ranges of temperature for all periods are shown in **Table 2**. The Cold Point Tropopause (CPT) maximum occured at evening/night, as shown in column 4 of **Table 2**. The value is quite similar with that was reported by Bhatnagar et al. [8]. CPT fluctuations do not show the trend of heating or cooling, due to limited data. The trend of CPT is important because at troposphere, it could provide an impact on stratosphere state. A positive trend has been found in stratospheric water vapour [15-16]. It was proposed that a warming trend was about 1° K/decade in tropical tropopause temperatures may explain the positive trend in stratospheric water vapour.

Table 2. Temperature range, maximum height and estimated height of tropopause on Radiosonde launch period

Launch time	Temperature range (°K)	Maximum height (km)	Cold point tropopause (CPT) height (km)
August 30th 2016, 08 LT	186.5-294.9	26.8	17.1
August 30th 2016, 11 LT	186.5-299.6	25.9	17.0
August 30th 2016, 15 LT	187.7-297.7	25.6	17.3
August 31th 2016, 07 LT	187.9-294.6	26.1	17.0
August 31th 2016, 11 LT	189.2-299.1	26.9	16.8
August 31th 2016, 19 LT	190.8-294.9	24.6	17.4
September 1st 2016, 07 LT	188.9-293.9	26.6	16.6
September 1st 2016, 10 LT	191.3-298.8	24.3	17.0
September 1st 2016, 15 LT	190.1-294.0	18.3	16.9
September 2nd 2016, 07 LT	190.1-293.6	25.5	17.0
September 2nd 2016, 11 LT	190.1-298.5	24.2	16.6
September 2nd 2016, 18 LT	190.5-294.2	20.7	17.0

On August 30th 2016, small variations (diurnal) occurred from the ground up to 17 km, approximately. Above the layer, there was a relatively large variation. The same feature was showed by temperature data on August 31st, but time variation over 17 km was much greater than that on August 30th. On August 31st, there was a clear difference in the 11:58º LT temperature profile. The temperature profile on September 1st showed similar features with that on August 30, but large variations occurred at 20

km and above. The temperature variation over time on September 2 is almost non-existent (**Figure 2**). Large variation at low stratosphere could relate to variation in ultraviolet radiation and ozone production.

From those results, we can use the mean of temperature profile as shown on **Figure 3** (left) as a standard deviation of less than <0.7°K at range of 1.8 km to 16.1 km. There was no significant different of standard deviation in relation to the time. The result suggested that the gap of the launch time is small. For accurate estimation, the standard deviation above the height (**Figure 3**, right) should be considered. High standard deviation was also found at the surface up to 1.6 km (unpublished data). These results are appropriate with those reported by Margit & Wolfgang [6] which showed that a standard deviation of the temperature of 0.005° to 0.5° at the tropopause. Homogenization correction did not apply for higher than 1°K error. The high error above 16 km was suggested to come from chemistry process (ozone production) and atmospheric dynamics activities.

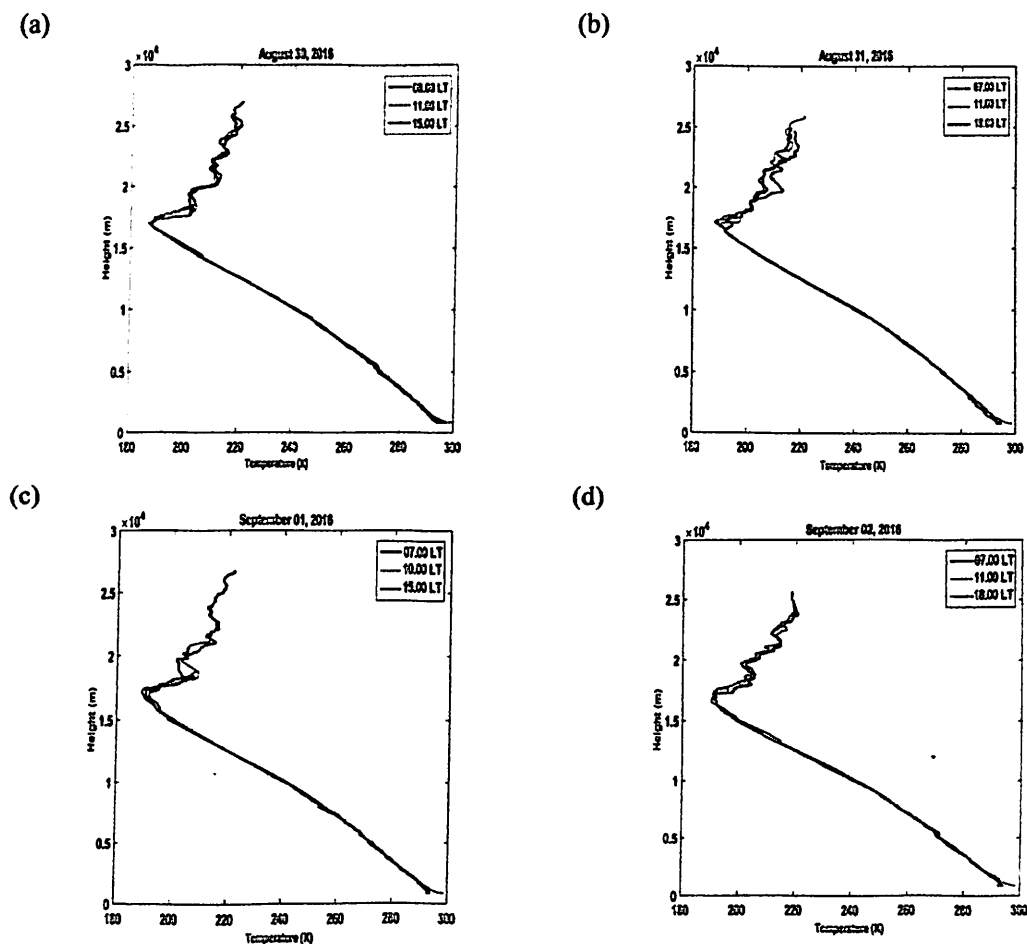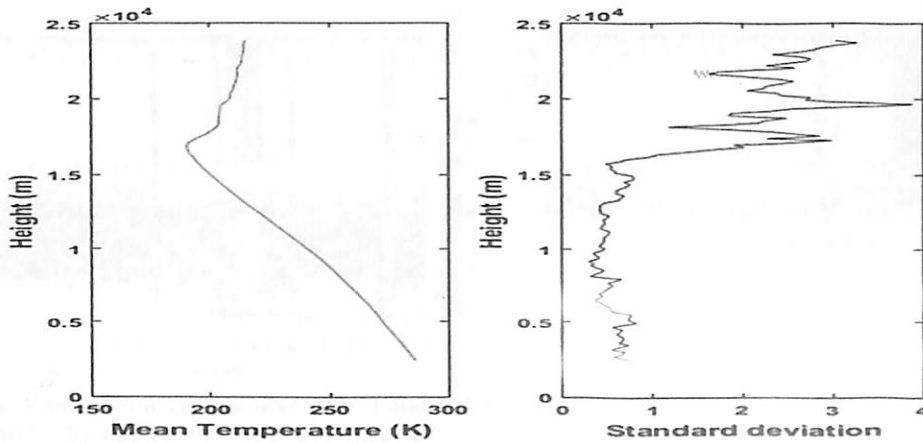(a)   (b)

(c)   (d)

Figure 2. Temperature profiles for: (a) August 30th, (b) August 31st, (c) September 1st and (d) September 2nd 2016

Figure 3. Profiles of mean temperature (left) and standard deviation (right) from 12 Radiosonde launch
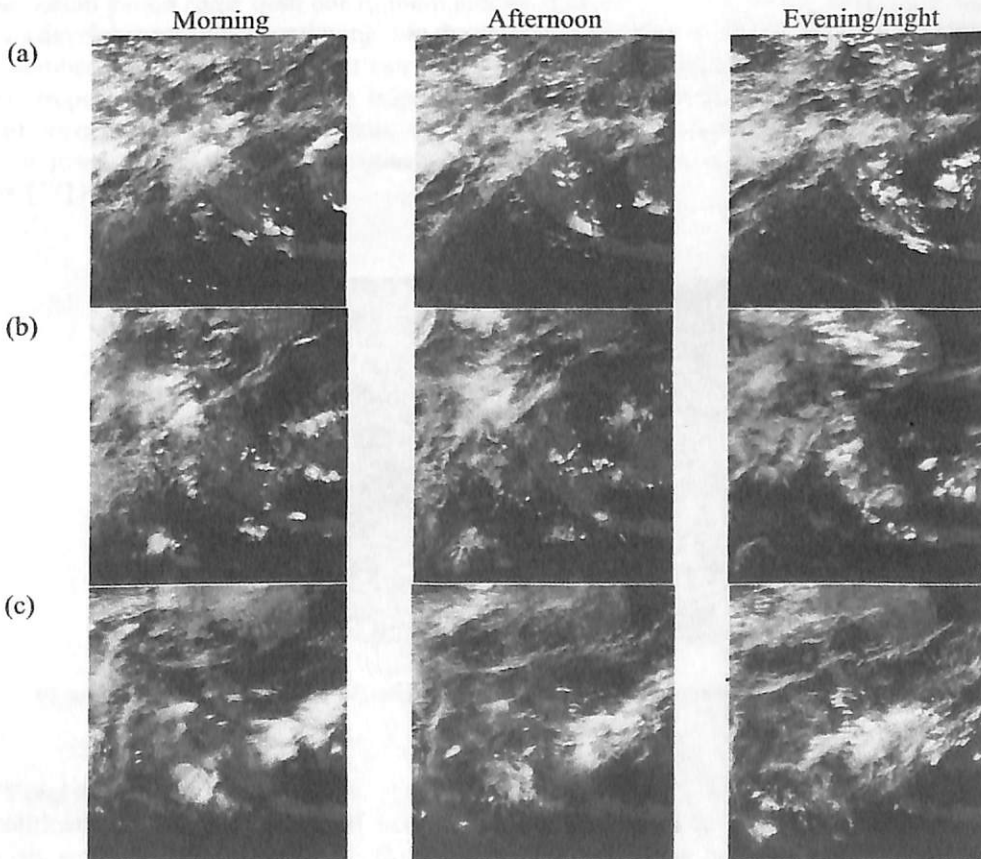
3.2 Rainfall

Based on MRR-2, rain occurred on all day observation in different intensity and duration. On August 30th, 2016, rain occurred since 14.00 Local Time (LT) until midnight as shown in **Figure 4**. Maximum intensity occurred at 14:00 LT-14:30 LT. Rain intensity decreased afterward. As shown on **Figure 4**, the rainfall took place on August 30th, August 31st, September 1st and September 2nd, 2016, respectively. The rain intensity and the radar reflectivity showed same pattern. Rainfall intensity on August 31st was lighter than August 30th, as well as the duration was shorter. The maximum of radar reflectivity at the time was over 30 dBz, deviated 10 dBz from rainfall on August 30th. The high intensity of rainfall recurred on September 1st and September 2nd, even though in shorter duration. On September 1st, rainfall occurred since morning, but maximum intensity occurred in between 12:00 to 13:00 LT. Rain stopped at 16:30LT and then fell again at 21:00 LT for an half-hour. Radar reflectivity had the same pattern with rainfall intensity and the maximum occurred at 12:30 LT was over than 40 dBz. On September 2nd, rainfall occurred since 14:00 to 15:30 LT. The rain fell again at 18:30 LT to 20:00 LT. The maximum of radar reflectivity maximum occurred at night.
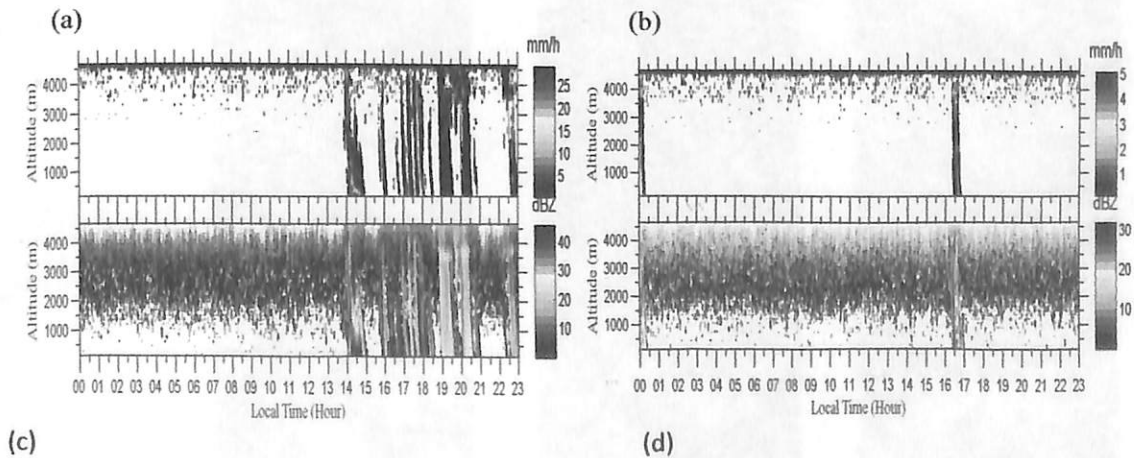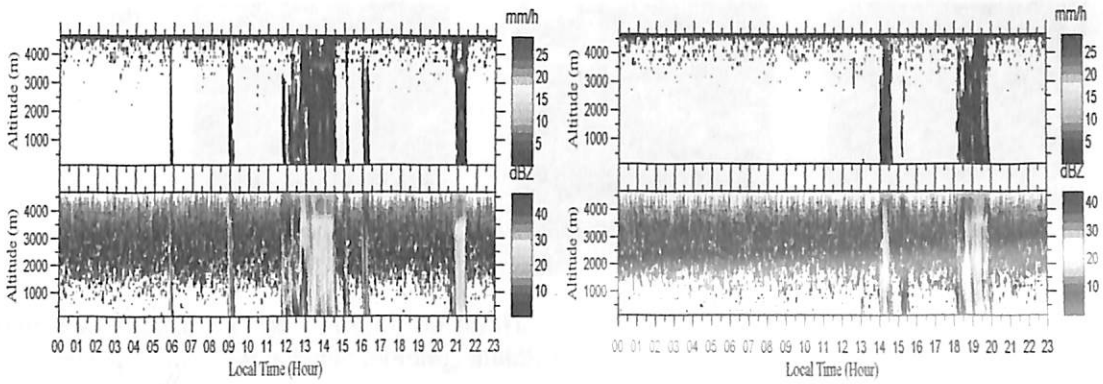
Figure 4. Rainfall intensity (above panel) and radar reflectivity (bottom panel) from MRR-2 for (a) August 30th, (b) August 31st, (c) September 1st, and (d) September 2nd 2016

Rainfall events that was detected by MRR-2 corresponded to HIMAWARI satellite images, as shown on **Figure 5**. The images time was adjusted to Radiosonde launch time and it turned out to coincide about two hours before the rain fell. The cloud covered the station during 4 days observation (**Figure 5**).

(d)
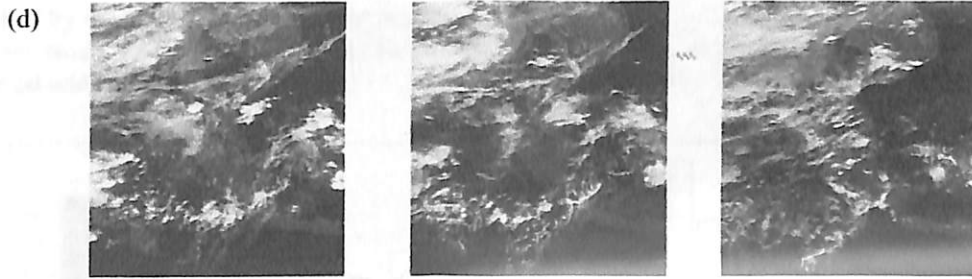
Figure 5. HIMAWARI IR-1 images for (a) August 30th. (b) August 31st , (c) September 1st and (d) September 2nd 2016 (left column: morning, middle column: afternoon, left column: evening/night)

3.3 Rainfall identification
3.3.1 Temperature deviation

Temperature deviation on **Figure 6** showed that the heating was mainly happened on August 30th and August 31st, while the cooling was on September 1st and September 2nd, 2016 from the surface up to 16 km. Above 16 km, the heating and the cooling had been quickly changing in higher intensity. The heating occurred when heat was released from the cloud or rain, while the cooling occurred when heat was absorbed from the environment. Radiosonde data could not be identified all the process, depending on the time resolution or the number of launch. Higher resolution data should catch the heating and cooling during each rain event. One thing can be deduced from the present study that rain during observation period came from one or more precipitation cell, and therefore, it indicated that the cloud and its developments were continuing into the second event after the first rainfall- and so on.

When the number of data is sufficient, it can be extracted to the stratosphere-troposphere coupling. Stratosphere-troposphere coupling at the tropopause was reported to be crucially important to the exchange of energy, momentum, and constituents such as H_2O and O_3 between the two regions [17]. Moreover, it plays a key role in the influence of stratospheric circulation on the QBO in the troposphere [18] PDO [19].
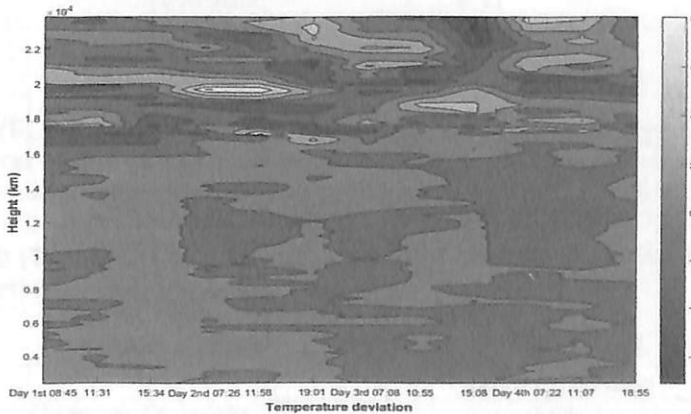
Figure 6. Temperature deviation from August 30th to September 2nd, 2016

3.3.2 CAPE and other Radiosonde indices

Rain identification was also performed using CAPE. Fluctuations in an intensity of rainfall as previously discussed correspond to CAPE fluctuations (**Figure 7**). The rain that occurred on August 30th at 14:00 LT was coincident with the CAPE value of >2000 Jkg^{-1} at 11:00 LT. Rainfall at 16:00 LT

was identified by the CAPE value of >5000 Jkg^{-1} at 15:00 LT. A low rain intensity on August 31st was identified by small CAPE (<2000 Jkg^{-1}). The same track can be applied for rainfall intensity on September 1st and September 2nd.
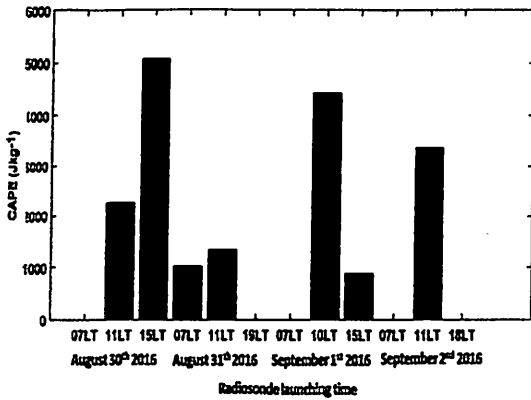

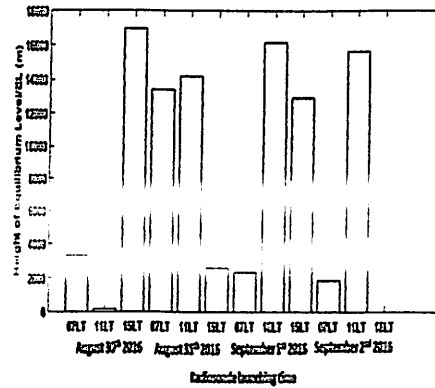**Figure 7.** CAPE estimation from Radiosonde data

Figure 8. Equilibrium level height

A strong relationship between CAPE (1-2 hours before the rain) and rainfall supported by the coefficient of correlation as shown in **Table 3**. The first row of **Table 3** indicates four of height classification of rainfall from MRR-2 data and the second row indicates coefficient of correlation between CAPE and MRR-2 rainfall for height classification. The maximum coefficient of correlation (0.85) appears at the third of height classification, from 3.2 to 4.5 km.

Table 3. Coefficient of correlation MRR-2 rainfall for different height and CAPE

Height (m)	Coefficient of correlation
150-1500	0.63
1650-3000	0.71
3150-4500	0.85
150-4500	0.80

Equilibrium level (EL) is the level above the level of free convection (LFC) at which the temperature of a rising air parcel again equals the temperature of the environment. The height of the EL is the height at which thunderstorm updrafts no longer accelerate upward. From Radiosonde estimation, the increasing of EQ altitude (**Figure 8**) is related to CAPE's values (**Figure 7**), as indicated by pattern correlation on 0.69 (**Table 4**). The coefficient of correlation of CAPE with EL temperature and EL pressure are also presented in **Table 4**.

Table 4. Pattern correlation between CAPE and EL

	Pattern correlation
CAPE vs EL height	0.69
CAPE vs EL temperature	-0.83
CAPE vs EL pressure	-0.76

4. Conclusions

This paper provides the latest temperature profile in the tropics and its relationship with Radiosonde indices based on 12 times Radiosonde launch. Radiosonde can reach the maximum height well enough on average over 25 km. The temperature profile varies over time with a standard deviation of 0.7.

Minimum temperature occurs in the morning while maximum temperature occurs in the afternoon. The relationship between rain and CAPE indicated the strong correlation. On the other hand, CAPE has a significant correlation with equilibrium level (EL), CAPE has a strong positive correlation with the height of EL and negative correlation with temperature and pressure of EL.

Acknowledgement

5. References

[1]   Xue-Long Z H, Marvin A. G and Minghua Z H 2001 Cooling trend of the tropical cold point tropopause temperatures and its implications *J. of Geophy. Res* 106 D2 1511-2

[2]   Peter W T, David E P, Simon F B T, Phil D J, Mark M, Holly C, and Philip B 2005 Revisiting Radiosonde upper air temperatures from 1958 to 2002 *J. of Geophy. Res* 110 D18105 doi:10.1029/2004JD005753

[3]   Melissa F and Dian J S 2005 Causes of differing temperature trends in radiosonde upper air data sets *J. of Geophy. Res.* 110 D07101 doi:10.1029/2004JD005481

[4]   David H D, John R C, Benjamin D P and S. Fred Singer A 2008 comparison of tropical temperature trends with model predictions *Int. J. Climatol.* 28 1693–01

[5]   William J R, Keith P S, John A, John B, Chantal C, Nathan P G, Philippe K, Ulrike L, Roger L, Craig L, Carl M, Alvin M, John N, Dian J S, David W J T, Fei W and Shigeo Y 2009 An update of observed stratospheric temperature trends *J. of Geophy, Res.* 114 D02107 doi:10.1029/2008JD010421

[6]   Margit PÁ and Wolfgang S 2015 Temperature Trends over Germany from Homogenized Radiosonde Data *J. Climate* 28 5699-15

[7]   Shoichiro F 2006 Coupling Processes in the Equatorial Atmosphere (CPEA):A Project Overview *J. of the Met. Soc. of Jpn* 84A 1-18

[8]   Bhatnagar, Panwar , Shibagaki , Hashiguchi, Fukao, Takahashi, Dhaka 2013 *Indian Journal of Radio & Space Physics* 42 277-91

[9]   Zapotocny, Jung, Le Marshall and Treadon 2008 A Two-Season Impact Study of Four Satellite Data Types and Rawinsonde Data in the NCEP Global Data Assimilation System *Weather and Forecasting, Volume* 23 80-100.

[10]   Gelaro and Zhu 2009 Examination of observation impacts derived from observing system experiments (OSEs) and adjoint models *Tellus A* 61 179-193

[11]   Laroche and Sarrazin 2010 Impact study with observations assimilated over North America and the North Pacific Ocean on the MSC global forecast system. Part I: Contribution of radiosonde, aircraft and satellite data *Atmosphere-Ocean* 48 10-25

[12]   Singh, Ojha, Kishtawal and Pal 2014 Impact of various observing systems on weather analysis and forecast over the Indian region *J. of Geophy. Res.: Atmospheres* 119 232-246

[13]   Kutty and Wang 2015 A Comparison of the Impacts of Radiosonde and AMSU Radiance Observations in GSI Based 3DEnsVar and 3DVar Data Assimilation Systems for NCEP GFS *Ad. in Met.* 2015 1-17

[14]   Michael P J , Donna J H, Petteri S, Raisa L, Shannon B, Tami T, and Karen L J 2016 Comparison of Vaisala radiosondes RS41 and RS92 at the ARM Southern Great Plains site *Atmos. Meas. Tech.* 9 3115–29.

[15]   Oltmans and Holmann 1995 Increase in lowerstratospheric water vapor at a mid-latidude northern hemisphere site from 1981 to 1994 *Nature* 374 146-9

[16]   Nedoluha, Bevilacqua, Gomez, Siskind, Hicks, Russell, and Conner 1998 Increases in middle atmospheric water vapor observed by the Halogen Occultation Experiment and the ground-based water vapor millimeter-wave spectrometer from 1991 to 1997 *J. Geophys. Res.* 103 3531-43.

[17]   James R H, Peter H H, Michael E M, Anne R D and Richard B R, and Leonhard P 1995 Stratosphere-Troposphere Exchange *Rev. of Geophy.* 33 403-39

[18]   Yasunari 1990 Impact of Indian monsoon on the coupled atmosphere ocean system in the tropical Pacific *Meteor. Atmos. Phys.* 44 29-41

[19]   Wuke W, Katja M, Nour-Eddine O and Mojib L 2016 Decadal variability of tropical tropopause temperature and its relationship to the Pacific Decadal Oscillation *Sci. Rep.* 6 29537 doi: 10.1038/srep29537